# Lab on a Chip

Accepted Manuscript

This is an *Accepted Manuscript*, which has been through the Royal Society of Chemistry peer review process and has been accepted for publication.

*Accepted Manuscripts* are published online shortly after acceptance, before technical editing, formatting and proof reading. Using this free service, authors can make their results available to the community, in citable form, before we publish the edited article. We will replace this *Accepted Manuscript* with the edited and formatted *Advance Article* as soon as it is available.

You can find more information about *Accepted Manuscripts* in the Information for Authors.

Please note that technical editing may introduce minor changes to the text and/or graphics, which may alter content. The journal's standard Terms & Conditions and the Ethical guidelines still apply. In no event shall the Royal Society of Chemistry be held responsible for any errors or omissions in this *Accepted Manuscript* or any consequences arising from the use of any information it contains.



ROYAL SOCIETY OF CHEMISTRY

www.rsc.org/loc

# Table of content entry

We present an ultra-fast microfluidic real-time PCR system enabling analysis in ≈7 minutes while conserving large volume and high efficiency/sensitivity.

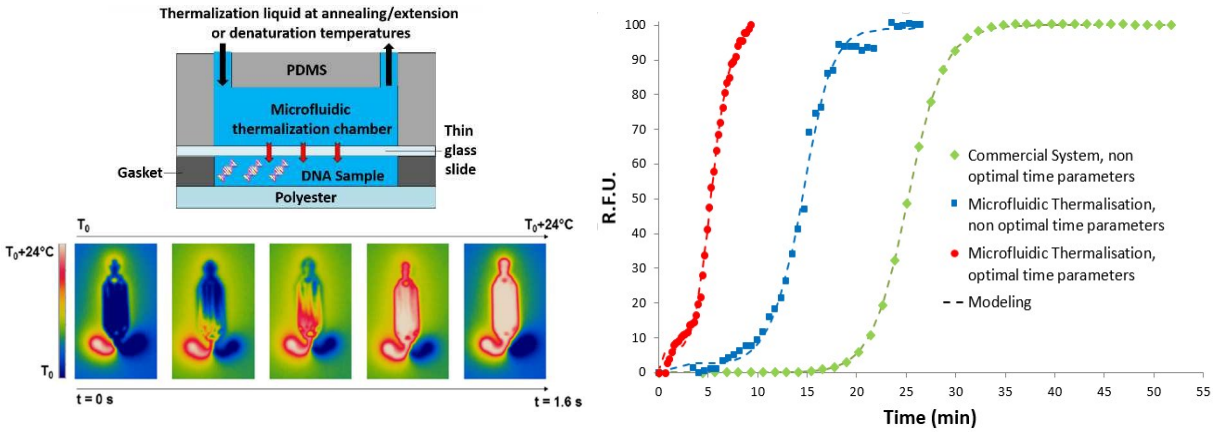


Lab on a Chip Accepted Manuscript

# *Ultrafast, sensitive and large-volume on-chip real-time PCR for the molecular diagnosis of bacterial and viral infections*

Timothée Houssin,‡*[a,b] Jérémy Cramer,‡[c,b] Rébecca Grojsman,[a] Lyes Bellahsene,[a] Guillaume Colas,[a] Hélène Moulet,[a] Walter Minnella,[a] Christophe Pannetier,[d] Maël Leberre,*[a] Adrien Plecis*[a] and Yong Chen*[b]

[a.] Elvesys - Innovation Center, 83 avenue Philippe Auguste, 75011, Paris, France. Tel: +33 (0) 1 84 16 38 06; E-mails: houssintimothee@gmail.com, mael.leberre@elvesys.com, adrien.plecis@elvesys.com

[b.] École Normale Supérieure-PSL Research University, 24 rue Lhomond, 75005, Paris, France. Tel: +33(0) 1 44 32 24 21; E-mail: yong.chen@ens.fr

[c.] Cherry Biotech, Université de Rennes 1, Campus Santé, Bât8, Et2, 2 Av. du Pr. Léon Bernard, CS 34317, 35043 Rennes Cedex ; E-mail : jeremy.cramer@cherrybiotech.com

[d.] Episteme Research and Consulting, 1 rue Rabelais, 92170, Vanves, France. Tel: +33(0) 6 60 43 85 36; E-mail: christophe.pannetier@epistemerc.eu

‡ These authors contributed equally to this work.

† Electronic Supplementary Information (ESI) available. See DOI: 10.1039/x0xx00000x

Lab on a Chip Accepted Manuscript

**Abstract**

To control future infectious disease outbreaks, like the 2014 Ebola epidemic, it is necessary to develop ultrafast molecular assays enabling rapid and sensitive diagnoses. To that end, several ultrafast real-time PCR systems have been previously developed, but they present issues that hinder their wide adoption, notably regarding their sensitivity and detection volume. An ultrafast, sensitive and large-volume real-time PCR system based on microfluidic thermalization is presented herein. The method is based on the circulation of pre-heated liquids in a microfluidic chip that thermalize the PCR chamber by diffusion and ultrafast flow switches. The system can achieve up to 30 real-time PCR cycles in around 2 minutes, which makes it the fastest PCR thermalization system for regular sample volume to the best of our knowledge. After biochemical optimization, anthrax and Ebola simulating agents could be detected in a 7-minute real-time PCR and a 7.5-minute reverse transcription real-time PCR (for 30 PCR cycles), respectively 6.4 and 7.2 times faster than with an off-the-shelf apparatus, while conserving real-time PCR sample volume, efficiency, selectivity and sensitivity. The high-speed thermalization also enabled us to perform sharp melting curve analyses in only 20s and to discriminate amplicons of different lengths by rapid real-time PCR. This real-time PCR microfluidic thermalization system is cost-effective, versatile and can be then further developed for point-of-care, multiplexed, ultrafast and highly sensitive molecular diagnoses of bacterial and viral diseases.

Lab on a Chip Accepted Manuscript

## Introduction

The 2014 Ebola outbreaks in West Africa demonstrated that fast, specific and sensitive diagnostic tools for effectively containing widespread epidemics are still lacking[1].

Indeed, rapid detection of viral infection currently relies mostly on immunoassays, such as the detection of antibodies specific to a viral infections or viral antigens developed on the surface of infected cells using the enzyme-linked immunosorbent assay (ELISA) in a strip format. This approach has been recently approved by the World Health Organization (WHO) for the detection of Ebola infection in 15-25 minutes[2].

Nevertheless, these types of assays still present several drawbacks: first, they are several orders of magnitude less sensitive than molecular assays and are thus not recommended for early diagnosis[3,4]. Furthermore, they may generate false positive results due to cross reactivity of other organisms that present the same antigen as the virus or elicit similar antibody responses[5]. In the case of the recent Ebola epidemic, this was particularly likely since Africans can present antibodies to pathogens like those causing malaria, tuberculosis and hepatitis, which obstruct results for Ebola detection, especially with field real samples[1].

For microbiological diagnoses (i.e. detection of bacteria, virus, fungi and parasites), the most reliable and sensitive methods rely on the real-time polymerase chain reaction (rtPCR) for DNA detection (e.g. for bacteria detection) and the reverse transcription real-time polymerase chain reaction (RT-rtPCR) for RNA analyses (e.g. for viral RNA detection)[6,7]. Nevertheless, these techniques typically last about one to three hours[8,9] and faster systems present drawbacks that will be discussed subsequently. Thus, the whole RT-rtPCR test for the diagnosis of the Ebola virus infection takes two to six hours[10]. Though this duration is a significant improvement over conventional culture-based microbiological assays, a faster diagnosis of epidemic diseases would enable healthcare providers to guide more efficiently the clinical decision for the improvement of treatment outcomes[10] and save more lives[1], especially when a large number of patients needs to be rapidly diagnosed and health care centers are overwhelmed[11].

Lab on a Chip Accepted Manuscript

The ideal diagnostic test must therefore combine the advantage of ELISA and rtPCR/RT-rtPCR for, respectively, faster detection and a more sensitive diagnosis. The WHO is therefore still looking for rapid assays enabling molecular diagnoses in less than 30 minutes to contain more efficiently Ebola virus outbreaks and more generally, other similar epidemics[10].

Regarding molecular amplification processes, new Droplet-rtPCR systems can be more sensitive than regular single-phase methods but assays also last longer (around 50% longer to ensure no temperature gradient through the droplet reservoir). Isothermal molecular amplification processes such as LAMP, NASBA, or RCA[12] are particularly interesting for point-of-care (POC) applications, but they remain relatively long (30-40 min)[13,14] and less flexible. Moreover, non-isothermal rtPCR relies on temperature cycles that allow matchless control of hybridization of primers to their cognate targets, so that it is essentially limited by thermalization ramps. In this regard, it is therefore possible to achieve ultrafast and non-isothermal rtPCR by accelerating thermalization speeds.

Previously, several ultrafast PCR and rtPCR systems (30 cycles in 2-15 min.) have been reported. For example, Moschou et al.[15] and Fuchiwaki et al.[16] developed respectively flow-through ultra-rapid PCR and rtPCR devices by displacing the sample between different temperature zones. In a similar manner, but without a fixed number of cycles, Brunklaus et al. used an oscillatory flow to perform ultrafast PCR[17]. Alternatively, by using a fixed PCR sample chamber exposed to temperature changes, i.e. static methods, Neuzil et al.[18] and Kim et al.[19] developed ultrafast rtPCR systems for nanoliter and biphasic samples using respectively thin films heaters and infra-red laser heating. Besides, Wheeler et al.[20] and Terazono et al.[21] used a liquid-based thermalization system method, close to the one presented herein, to demonstrate respectively ultrafast PCR and rtPCR-based detection.

Among industrial systems, BJS Technology recently commercialized the ultrafast XXpress rtPCR system, which can achieve 40 rtPCR cycles in 8-10 minutes[22]. Samsung developed the GenSpector systems based also on the Joule effect[23] with silicon heater that can detect the sacbrood virus in 22 minutes in a 1 µL sample[24] with off-chip RNA reverse transcription (RT). Analytik Jena commercializes the qTower which enables analyses in around

Lab on a Chip Accepted Manuscript

25 minutes with a volume range of 5 to 20 µL[25]. NanoBioSys developed an ultrafast rtPCR system which can reach 30 cycles in 15 minutes from a15 µL sample with a conserved efficiency and sensibility but off-chip RT as well[26]. Cepheid proposes the GeneXpert system that can carry out automatically sample preparation and multiplex rtPCR in approximately one hour[27].

All these systems showed interesting results for ultrafast rtPCR but present also disadvantages that limit their practical applications.

First, regarding sample volume, large systems present high thermal inertia and potential temperature inhomogeneity. Indeed, temperature differences of up to +/- 65°C could be observed during the transient time with conventional rtPCR systems using multi-well plates[28] (typical volumes of 20-25 µL). Whereas, it is important to maintain a good thermal homogeneity throughout the reaction to ensure the best rtPCR efficiency[29–32] and specificity[33]. For the ultrafast PCR and rtPCR systems listed above, the use of smaller sample volumes thus facilitates faster thermalization and a better temperature homogeneity but decreases intrinsically the system sensitivity (or limit of detection, i.e. the minimum detectable copy number). Indeed, low-volume rtPCR chambers will more likely yield no amplifications due to the initial absence of DNA targets in low-concentration samples used in sensitive detections (e.g. from saliva and ocular samples[34]) caused by the stochastic variation of sample copy number with Poisson distribution[35,36]. Furthermore, a larger reaction chamber also enables the integration of complementary operations for POC PCR analysis in the same PCR chamber[34]: e.g. DNA solid phase extraction through alumina nano-membranes[37] or dry-stored PCR reagents in paraffin[38,39].

Regarding flow-through systems, they present the disadvantage of not being flexible about the number of PCR cycles, which is fixed by the device design. This drawback can be avoided by using an oscillatory flow design but, to our knowledge, this type of system has not been used for real-time amplification detection. Noteworthy, flow-through systems can be used for melting curve analyses like static rt-PCR systems as shown by Crews et al.[40]. Finally, both

Lab on a Chip Accepted Manuscript

flow-through and oscillatory flow systems complicate the straightforward adjustment of PCR phase times and sample volumes.

Lastly, for all the above-mentioned systems (except for the GeneXpert), the sensitivity and/or amplification efficiency was either decreased compared to commercial PCR-rtPCR systems or not characterized.

Other works also presented ultrafast PCR systems (25-30 cycles in 2-6 minutes), but are not applicable yet to more sensitive real-time detections (i.e. rtPCR)[15,17,20,41,42].

The system presented here aims to increase drastically the rtPCR thermalization speed and to improve temperature homogeneity while conserving the advantage of conventional rtPCR systems i.e. a high efficiency/sensitivity associated with a large reaction volume (20-25 µL).

This ultrafast rtPCR system consists of a liquid-based thermalization system using a transparent microfluidic device associated with high speed microfluidic switches (i.e. microfluidic thermalization). These nearly instantaneous injections, associated with the improved thermal conduction of liquids compared to air and the large surface to volume ratio inherent to microfluidics, enables thermalization speeds up to 8 times faster than regular air thermalization and a perfect temperature homogeneity. Thus, we achieved rtPCR-based bacteria detections in 7 minutes while displaying sensitivity and efficiency very similar to conventional rtPCR systems and RT-rtPCR-based viral analyses in 7.5 minutes, both assays being carried out within regular 25 µL sample volumes. Our system is thus compatible with a broad range of sample volumes from nanoliters to tens of microliters and therefore, with applications requiring excellent limit of detection.

The microfluidic device and system are first described. The rtPCR and RT-rtPCR protocols as well as the rtPCR curve modeling are then presented. Thermalization performances have been characterized. rtPCR and RT-rtPCR durations have been optimized and compared to those of a commercial rtPCR system using anthrax (bacteria) and Ebola (virus) simulating agents. rtPCR sensitivity and efficiency have been determined and

Lab on a Chip Accepted Manuscript

compared as well. Precise melting curve analyses are then obtained in a few seconds. Finally, the discrimination of different amplicon lengths by ultrafast rtPCR is demonstrated.

Lab on a Chip Accepted Manuscript

## Experimental

*rtPCR device and microfluidic thermalization*

The microfluidic device used in this work consists of two chambers separated by a 170 µm thick glass slide (Corning cover glass, Corning) which serves as a thermal bridge. The upper chamber made of polymethylsiloxane (PDMS, RTV 615, Eleco Products), was fabricated by conventional soft-lithography techniques[43] and is used for flow-controlled thermalization. This large thermalization chamber is supported by PDMS micropillars to avoid its collapse. The lower chamber of 25 µL, made of adhesive polyester (Gene Frames, Thermo scientific), was bonded to the glass slide, allowing a biochemical reaction with a comparable sample volume as that of 96 well-plates for conventional rtPCR. The glass surface in contact with PCR samples was passivated with PII-g-PEG (PII(20)-g[3.5]-PEG(2), 0.1 mg/mL, SUSOS) to avoid adsorption of PCR reagents.

The microfluidic thermalization technique consists in alternatively injecting two pre-heated liquids corresponding to the annealing/elongation temperatures or the RT one (i.e. 60, 64, 72, or 50 °C respectively) and the denaturation temperature (i.e. 96 °C) in the upper chamber through two distinct inlets (Fig. 1a). After the thermalization chamber, the pre-heated liquids exit from a common outlet (Fig. 1b). The temperature time course is calibrated with an infrared thermometer (Optris CS LT, Acoris) (Fig. 1c), while the temperature homogeneity is characterized with an infra-red camera (Optris PI 160, Acoris), both measuring the temperature of the external side of the glass slide underneath the microfluidic chip, i.e. the glass slide side in contact with the biological sample.

*Ultrafast rtPCR system*

The whole rtPCR system (Fig. 1d) consists of a temperature controller with two heat exchangers (adapted from the Cherry Temp system, Cherry Biotech). These heat exchangers adjust the temperatures of heat-transfer liquids injected into the thermalization chamber in order to obtain the two desired rtPCR temperatures.

Lab on a Chip Accepted Manuscript

The two heat transfer fluids (LIQ-702, Koolance, i.e. ≈ 25% propylene glycol and 75% distilled water), are sequentially transferred from two glass reservoirs (500 mL Bottle media, Fisher Scientific) into the heat exchangers and then into the thermalization chamber and their flow is controlled with a pressure controller (OB1 MkII, Elveflow).

The two fluids are continuously heated and sequentially injected from the reservoirs through microfluidic caps (100 mL Large Microfluidic Reservoir Kit, Elveflow) via flexible tubing (Microfluidic 1/16-23G Tygon Tubing Kit, Elveflow).

The fluorescence detection is carried out by a fluorescence measuring system (Fluoreader, Elveflow) placed under the microfluidic device and its PCR chamber (Fig. 1e).

The pressure control and fluorescence detection are synchronized by an Elveflow Matlab script (Mathworks) and the temperature control is managed by the Cherry Temp software (Cherry Biotech).

The whole system weighs less than 10 kg making its potential adaptation to POC detections readily conceivable.

*PCR, rtPCR and RT-rtPCR protocols*

For PCR & rtPCR assays, DNA extracted and purified from *Bacillus atrophaeus* subsp. *globigii* (BG) bacteria (Directorate General of Armaments (DGA), CBRN Defense) was used. For each assay, 125 ng of genomic DNA were used except when otherwise specified. Two different rtPCR master mix kits were used at a 1X concentration: Sso Advance Universal SYBR Green Super Mix (Biorad) for SYBR Green assays and QuantiFast Probe PCR + ROX Vial Kit (Qiagen) for probe assays.

For RT-rtPCR assays, extracted and purified MS2 virus RNA was amplified (DGA, CBRN Defense and Roche). For each assay, 100 ng of initial RNA were used except when otherwise specified. QuantiFast Probe RT-PCR + ROX vial Kit (Qiagen) was used as a master RT-rtPCR mix at a 1X concentration for probe assays.

All oligonucleotides (primers and probes) were purchased from DGA, CBRN Defense and Eurogentec. Amplicons sequences and characteristics are presented in table S1 (ESI†).

Lab on a Chip Accepted Manuscript

For PCR and rtPCR, primers and probes were used at a concentration of 500 and 100 nM respectively. For RT-rtPCR, primers and probes were used at a concentration of 800 and 200 nM respectively.

For PCR, rtPCR and RT-rtPCR, a denaturation temperature of 96 °C was used. For PCR and rtPCR, the annealing/elongation temperature was optimized by a PCR temperature gradient assay (Fig. S1, ESI†) and, a temperature of 64 °C was then chosen. For RT-rtPCR, reverse-transcription and annealing/elongation temperatures of respectively 50 °C and 60 °C were used. The durations of the different rtPCR and RT-rtPCR phases were optimized (see Results and methods).

For molecular assays done in microfluidic devices, the Geneframe frame was first bonded to the glass substrate of the microfluidic device, under the thermalization chamber, by 5 min heating at 95 °C (through liquid thermalization). Then 40 µL of rtPCR and RT-rtPCR mixes were prepared, thoroughly mixed and pipetted onto the glass substrate. The 25 µL Geneframe chamber was then sealed with the polyester coverslip. The overflowing mix was then carefully removed by capillarity through a clean-room paper sheet. The microfluidic device containing the DNA sample was then placed into the rtPCR set-up, above the fluorescence detector, and connected to the heat exchangers and outlet reservoir via microfluidic tubes. The microfluidic device and the fluorescence detector were placed into an opaque box to avoid ambient optical noise. The assay was then started and automatically managed via the Elveflow Matlab script. For rtPCR assays with the microfluidic device, rtPCR and RT-rtPCR phases times mentioned take into account the thermalization times.

For comparative PCR and rtPCR assays done in conventional commercial systems, a $^{3}$prime thermal cycler (Techne) with 0.5 mL tube and a Light Cycler 480 (LC480, Roche) with 96 well plates were respectively used, keeping the same reagent concentrations and mix volumes as for the assays in microfluidic devices. For assays in the LC480, the rtPCR and RT-rtPCR phases times mentioned do not include the thermalization times.

For the determination of rtPCR sensitivity with 100 genomic DNA copies, the initial DNA stock was serially diluted into a salmon sperm DNA solution at 100 µg/mL (UltraPure Salmon

Lab on a Chip Accepted Manuscript

Sperm DNA Solution, Life Technologies) used as carrier DNA instead of deionized (Milli-Q) water to avoid the loss of material due to non-specific DNA binding during dilution or on the sample chamber surfaces.

*Melting curve analysis with the microfluidic device*

For the melting curve analysis, the temperature in one of the heaters was ramped up from 70°C to 90°C while exposing the microfluidic chamber to the heat transfer fluids from this heater. The thermal kinetic was first characterized with the infrared thermometer and the fluorescent measurement from the melting curve assay was then correlated with this thermal kinetic to obtain the melting curve from the microfluidic device.

*Numerical simulation and rtPCR curves fitting*

The speed of microfluidic thermalization was analyzed using multiphysics modeling (Comsol, France).

The cycle threshold (Ct) for rtPCR and RT-rtPCR was determined by amplification curves fitting the following 5 parameters log-logistic model[44]:

$$\mathbf{g}(\mathbf{x}, \mathbf{b}, \mathbf{c}, \mathbf{d}, \mathbf{e}, \mathbf{f}) = \mathbf{c} + \frac{\mathbf{d} - \mathbf{c}}{(\mathbf{1} + \mathbf{e}^{\mathbf{b}(\log(\mathbf{x}) - \log(\mathbf{e}))})^{\mathbf{f}}}$$

After rtPCR curves fitting, a 2nd derivative maximum method[45] was used to determine the Ct.

Lab on a Chip Accepted Manuscript

## Results and discussion

*Thermalization performances*

The speed of microfluidic thermalization was first optimized according to the results of a numerical simulation, which showed that higher flow rates enabled faster thermalization speeds but also a stable plateau for repeatability (Fig S2, ESI†).

Then, the maximum flow rate that the rtPCR system could withstand at PCR temperatures was first assessed. For flow rate ≥ 18 mL/min, the heating exchangers could not sufficiently heat the carrier liquids so that 17 mL/min was considered as the upper flow rate limit ensured to remain on the thermalization plateau (low influence of flow fluctuations on temperature control). With this flow rate and a temperature switch between 72 and 98 °C (typical rtPCR temperatures used for commercial rtPCR kits), the microfluidic thermalization could achieve 30 cycles in ≈ 2 min (127.5 s) (Fig 2.a), i.e. 4.25 s per cycle. To the best of our knowledge, this makes it the fastest static (i.e. unlike flow-through or oscillatory methods) rtPCR thermalization system using regular sample volume. At this speed, the annealing/elongation (between 72 and 75 °C) and denaturation (above 95 °C) plateaus lasted 1.05 s and 0.5 s respectively. The maximum heating ramp rate was 25 °C/s and the maximum cooling ramp rate was 18 °C/s. For comparison, the shortest rtPCR assays achievable with a commercial system for 30 rtPCR cycles with 30s initial denaturation, 1s denaturation and 1s annealing/elongation lasted 18.4 min. Thus, our microfluidic thermalization system enables a rtPCR cycling that is 8.7 times faster than conventional ones.

The microfluidic thermalization also enabled a better thermal homogeneity of the PCR samples during each temperature cycles despite a large volume. Indeed, the results of infrared imaging showed a temperature homogeneity of 0.03 °C (maximum temperature difference) during ultrafast thermalization (less than 2s for cooling).

After optimization of the thermal performances, we carried out an ultrafast rtPCR of BG DNA through temperature cycling between 64 and 96 °C with a SYBR Green reporter, but no exponential amplification occurred. This might be explained by the fact that rtPCR cycles, notably the annealing-elongation step, were too short. Indeed, the shortest annealing times

Lab on a Chip Accepted Manuscript

described last around 1 s[46]. Then, the Sso7d fusion DNA polymerase used in the SYBR Green rtPCR master mix (see Materials and Methods) has a polymerisation rate of 100 bases per sec. in optimal conditions. Thus, the 1 s annealing/extension around 64°C might not be long enough for the primers annealing and the complete amplicons extension.

*Determination of optimal amplification parameters*

To confirm the specificity of the amplification process in the presence of SYBR Green, PCR amplification with a SYBR Green mix has been carried out in the microfluidic device and a thermocycler, followed by a DNA electrophoresis analysis which shows that expected specific amplicons have been obtained (Figure S3, ESI†).

To reduce rtPCR and RT-rtPCR durations while maintaining amplification efficiency, we achieved a dichotomous reduction of rtPCR time parameters validated with the conservation of Ct for both reporters (probes and SYBR Green). Thus, this Ct was first determined with a commercial rtPCR system (cf material and methods) and the microfluidic device using recommended rtPCR times (180 s for initial denaturation, 5 s for denaturation and 30 s for annealing/elongation time) and BG DNA to validate our rtPCR system in regular conditions.

The initial denaturation time was then first reduced, secondly the denaturation time was decreased, and finally, the annealing/elongation time was diminished. The dichotomous reduction of rtPCR time parameters and its different results is presented in detail in the table S2 (ESI†). The results obtained for the annealing/elongation time reduction with both reporters are represented in the Fig. 3a.

As it can be seen, for both SYBR Green and probe reporters, Ct is first conserved or slightly decreased as the annealing-elongation time is progressively reduced before increasing. This Ct increase for shorter elongation times can be explained by the fact that DNA polymerases have less time to replicate DNA amplicons and thus partially replicate them. It can also be explained by the fact that primers/probes or SYBR Green do not have the time to bind with DNA targets or double-stranded DNA respectively. This maximal rtPCR speed for ultrafast rtPCR has also been observed previously[18]. The shorter annealing-elongation time

Lab on a Chip Accepted Manuscript

obtained with probes compared to SYBR Green is consistent with the observation that DNA intercalating dyes like SYBR Green decrease the polymerase polymerization rate[47].

To obtain the lowest cycle thresholds while maintaining state-of-the art sensitivity, we could select the following rtPCR optimized time parameters:

- 30 s for the initial denaturation, 3 s for the denaturation and 8 s for the elongation with probes, i.e. 6 minutes for 30 rtPCR cycles.
- 30 s for the initial denaturation, 3s for the denaturation and 10 s for the elongation with SYBR Green, i.e. 7 minutes for 30 rtPCR cycles.

Compared to the commercial rtPCR system (cf table S2, ESI†), we also observed that the rtPCR cycle thresholds obtained with probes and the microfluidic thermalization are lower (from 14.55 to 12.27 cycles with the microfluidic thermalization and 15.89 with the commercial rtPCR system). On the contrary, the rtPCR cycle thresholds obtained with SYBR Green and the microfluidic thermalization are first higher, but reach the same order when annealing/elongation time is reduced (from 16.34 to 15.26 with the microfluidic thermalization and 14.93 with the commercial rtPCR system).

By comparing rtPCR curves with probes and SYBR Green for regular (30 s) and fast (8-10 s) annealing-elongation phases (cf Fig. 3b), it can be noticed that fast and regular rtPCR curves for both reporters have the same Ct but different exponential phase slopes and thus, different final fluorescence intensities. These differences can be explained by the fact that the amplification efficiencies are identical during the first cycles, when reagents are in excess, and therefore yield highly similar Ct. When the number of amplicons increase exponentially in the following exponential phase with a constant amount of DNA polymerase, DNA polymerases need to amplify more DNA amplicons with the same efficiencies during the same annealing-elongation phase time, which may not be possible with fast and shorter annealing-elongation phases. This decrease of efficiency in ultrafast PCR when the ratio of polymerase to targets decreases also sustains that in the present experimentations, the binding of the polymerase became the limiting factor in term of rtPCR rapidity. Furthermore, when the number of amplicons increases exponentially after the Ct, single-stranded complementary amplicons

Lab on a Chip Accepted Manuscript

compete with primers for hybridization[48,49], which decreases amplification efficiency in late PCR cycles, especially with short annealing-elongation phases. Most importantly, this effect does not influence the cycle threshold determining the amplification efficiency and system sensitivity.

It can also be seen that the fast rtPCR curve obtained with probes has no plateau phase like it is the case for regular rtPCR curves, the ones obtained with regular annealing-elongation phases and the one obtained with SYBR Green and fast annealing-elongation phase. Therefore, to keep the same regular rtPCR amplification behaviour presenting saturation phases, only SYBR Green reporters have been used for the subsequent rtPCR assays. We assume this biochemical phenomenon related to the amplification speed could be explained by the fact that, when the number of amplicon increases exponentially after the Ct,

single-stranded complementary amplicons compete with primers but also with probes for hybridization[48,49], unlike SYBR Green that binds to single-stranded or double-stranded DNA regardless of potential hybridization[50]. Thus the probes are maintained in excess, unlike SYBR Green, causing no plateau phase.

To assess whether this fast amplification is also applicable to RNA targets, RT-rtPCR has been carried out in the microfluidic device with MS2 RNA. Using regular time parameters (600 s RT, 300 s initial denaturation, 10 s denaturation, 30 s annealing/elongation, i.e. 35 min for 30 RT-rtPCR cycles), a Ct of 10.88 was obtained (Fig S4, ESI†). By reducing the RT duration 20 fold, the Ct only varied from less than 1 cycle (600 s: Ct = 9.45, 30 s: Ct = 10.3) (Fig. 3c). After optimization, we achieved an on-chip RT-rtPCR of 30 cycles in 7.5 minutes with a Ct of 7.84 (30 s RT, 30 s initial denaturation, 3 s denaturation, 10 s annealing/elongation, i.e. 7 minutes 30 s for 30 RT-rtPCR cycles) (Fig S5, ESI†). It can be noticed that the ultrafast RT-rtPCR curves obtained with probes also presented no plateau phase like the ultrafast rtPCR curves obtained with probes.

*Performance comparison of microfluidic rtPCR and RT-rtPCR with conventional system*



Lab on a Chip Accepted Manuscript

Time optimization with our device could have been obtained at the expense of PCR efficiency. To assess whether this was the case, we compared the rtPCR and RT-rtPCR amplification efficiency from our microfluidic device to that of a state-of-the-art commercial (real-time) thermal cyclers (cf Experimental).

First, we compared rtPCR and RT-rtPCR amplification efficiencies with both systems under non-optimized time conditions and with the microfluidic device under optimized time conditions (Fig 4.a & b, respectively).

It can be seen that rtPCR durations can be reduced from 40 min for 30 cycles with the commercial rtPCR system to 20.5 min with the microfluidic chip and non-optimized time parameters and further down to 7 min with optimized time parameters (Fig 4.a), i.e. a molecular detection of anthrax simulating agent that is 5.7 times faster. Likewise, RT-rtPCR durations could be reduced from 54 min for 30 cycles with the commercial rtPCR system to 35 min with the microfluidic chip under non-optimized time parameters and further down to 7.5 min with optimized time parameters (Fig 4.b), i.e. a molecular detection of Ebola simulating agent that is 7.2 times faster.

It is important that the reduction in rtPCR and RT-rtPCR durations does not compromise amplification efficiency, which is critical for sensitive molecular detections. So we characterized rtPCR amplification efficiencies with the standard curve method by measuring the Ct from sample serial dilutions with the commercial rtPCR system and the microfluidic thermalization systems (same samples analyzed in parallel with both systems) (Fig 4.c). It can be noted that amplification efficiencies obtained were almost identical with a 5% variation between standard curves slopes. Therefore, the amplification efficiency obtained with the commercial rtPCR system was conserved with our microfluidic thermalization system, though the rtPCR assay duration was decreased by more than 6 times.

In the previous optimization experiments, we had used rather high numbers of DNA copies (in the range of 27 million copies for rtPCR). Having made sure that the efficiency was maintained for these number of targets, we next wanted to assess the sensitivity, i.e. the lowest detectable amount of initial DNA copies, achievable with our system. It has been previously

Lab on a Chip Accepted Manuscript

shown that the sensitivity of Light Cycler systems is around 100 copies for a close to 100 % probability of detection[51,52]. Therefore, we chose to assess whether the limit of detection of our microfluidic thermalization system was comparable. To do so, we serially diluted BG DNA samples in a salmon sperm DNA solution instead of purified water, as described in the material & methods section, in order to avoid loss of DNA by non-specific DNA binding during the dilution process and/or on the sample chamber surfaces. Using the same optimized protocol, we were able to detect as few as 100 initial copies of BG DNA within 7 min without observing a reduction of the rtPCR amplification efficiency (cf Fig 4.c), thus obtaining a sensitivity comparable to the state-of-the-art systems (our primers target a DNA sequence that is present only once in the BG genome). To confirm that this result was not due to sample contamination, we carried out a negative control in parallel by replacing the initial DNA sample with purified water. As expected, compared to the rtPCR curve obtained for 100 initial BG DNA copies, no amplification occurred (Fig S6, ESI†).

Concerning the amplification efficiency of ultrafast RT-rtPCR, it can be noted also that the RT-rtPCR carried out in 7.5 minutes for 30 rtPCR cycles (9.67 minutes for 40 rtPCR cycles) with the microfluidic device presents a Ct of 7.84 (cf previous paragraph and Fig S5, ESI†) equivalent to the Ct of 7.72 +/- 0.16 obtained with the commercial rtPCR system in 66.75 minutes for 40 cycles i.e. in a duration 6.9 times longer than with microfluidic thermalization.

*Ultrafast melting curve analysis*

For molecular assays using intercalating dyes like SYBR Green, melting or dissociation curve analysis is required to ensure the specificity of the amplification since these dyes will interact with any double stranded DNA like primer dimers and non-specific products. Interestingly, melting curve analysis can also be used with probes like molecular beacons, for the identification of single-nucleotide polymorphisms[53] (SNPs) for instance. Melting curves are obtained by exposing the resulting rtPCR product to a temperature increase and monitoring in parallel the resulting fluorescence. If a single peak can be observed at the expected

Lab on a Chip Accepted Manuscript

temperature value on the first negative derivative of the fluorescence as a function of the temperature, the amplification is confirmed to be specific.

Therefore, we used the microfluidic thermalization system to carry out an ultrafast temperature modification for melting curve analysis (fig 5).

The assay was carried out in only 20s and its derivative showed a single peak, demonstrating thus a specific rtPCR amplification. Melting temperatures for the BG amplicons should be comprised between 75 °C and 81 °C according to two different rtPCR software[54,55] so the obtained experimental melting temperature of 77.5 °C corresponds to the theoretical results. Interestingly, the Full Width at Half Maximum (FWHM) for the derivative of this melting transition is very narrow: 1.7 °C. This sharp melting transition is an important property for high-resolution melting curves and, thus, the discrimination of different amplicons and SNPs[56]. Therefore, interestingly, our microfluidic system is able to perform fast and sharp melting curve analyses, which is in agreement with the achieved temperature homogeneity that we noted previously.

*Amplicon length discrimination with ultrafast rtPCR analysis*

For unknown pathogen detection and other applications, multiplex rtPCR is a critical technology that is still hindered by the unexpected formation of non-specific PCR products due notably to too long elongation phases[57]. Ultrafast rtPCR and its short elongation phases could be naturally endowed with the ability to distinguish relevant short amplicons from unwanted long non-specific amplicons. To demonstrate this feature, 65-bp long BG amplicons and approximatively 10 times longer (500bp) BG amplicons were therefore analyzed by ultrafast rtPCR within the microfluidic device to study whether their distinction was possible. For this purpose, for each type of amplicon length, two rtPCRs were carried out with different annealing-elongation phase times: a short (10 s) and a long one (30 s) (fig 6).

As observed and explained previously (cf fig 3), the rtPCR with short and long annealing-elongation phases for the 65-bp amplicons have identical Ct (respectively 15.26 and 15.24) but different exponential phase slopes and final fluorescence values.



Lab on a Chip Accepted Manuscript

The rtPCR with long annealing-elongation phases for the 500-bp amplicons have a higher Ct of 20.28 whereas the initial DNA concentrations were the same. This could be explained by a decreased amplification efficiency due to the longer amplicons length. As expected, no exponential amplification occurred for these longer 500-bp amplicons with short annealing-elongation phases i.e. in ultrafast rtPCR conditions, unlike shorter 65-bp amplicons.

This lack of amplification of 500-bp amplicons with short annealing-elongation phases can be explained by the previously mentioned biochemical phenomenon, i.e. DNA polymerases overwhelmed by amplicon numbers in short annealing-elongation times and single-stranded complementary amplicons reannealing. Both phenomena would be further improved with long amplicons amplified during short annealing-elongation times and would so happen here as soon as the first PCR cycles (before Ct), totally preventing any DNA amplification. As mentioned before, since SYBR Green decreases polymerase polymerization rate, the polymerase polymerization rate would be further slowed down for these longer amplicons[47].

Therefore, the minimum annealing-elongation phase time for 500-bp amplicons could also be optimized step-by-step as we previously did for shorter amplicons (cf fig. 3.a.). Nevertheless, in the optimal ultrafast rtPCR conditions for 65-bp amplicons, these latter can be efficiently amplified, unlike 500-bp amplicons.

It is therefore demonstrated here that ultrafast rtPCR can be used to selectively amplify shorter specific amplicons and intrinsically prevent the amplification of non-specific products, presumably longer as they would result from rare mis-priming events. Speed could therefore improve the detection specificity of rtPCR in noisy environments, potentially reducing both false positive and false negative rates due to interference with larger sequences.

Lab on a Chip Accepted Manuscript

## Conclusion

We have developed an ultrafast rtPCR system using microfluidic thermalization that enables the carrying out of 30 rtPCR cycles in only ≈ 2 minutes with regular microliter size samples (25 µL) and a 0.03°C thermalization homogeneity. This result makes the microfluidic thermalization technique the fastest and most homogeneous static rtPCR thermalization system using regular sample volume to our knowledge. These ultrafast cycles enabled us to precisely test the limits of primer annealing and elongation activity required for successful DNA exponential amplification. By progressively reducing the rtPCR cycle durations while checking for the amplification efficiency conservation, we were able to detect anthrax simulating agents by rtPCR in 7 minutes and Ebola simulating agents by RT-rtPCR in 7.5 minutes (30 cycles for both detections), i.e. respectively 5.7 and 7.2 times faster than a commercial rtPCR system. Compared with the conventional system, ultrafast rtPCR detection was carried out with the same efficiency and sensitivity, thus showing no trade-off between speed and detection performances. The high-speed thermalization also enabled us to perform ultrafast melting curve analyses in only 20 s with a sharp melting transition (FWHM of only 1.7 °C). Finally, different amplicon lengths could be distinguished by ultrafast rtPCR: shorter amplicons (65 bp) can be amplified unlike longer ones (500 bp). This discrimination method could be relevant to reducing sequence interferences especially in multiplex rtPCR format.

The microfluidic thermalization technology reported in this work has been demonstrated as an innovative and cost-efficient process for ultrafast rtPCR and RT-rtPCR and notably their applications for rapid and specific molecular detection of bacteria and viruses. Indeed, the design of the device includes microfluidic networks that can be produced at low cost by standard polymer molding technologies. To develop a system for complete ultrafast molecular diagnosis, the above described rt-PCR system has to be associated with an equally fast sample preparation process, whose development will be undertaken in the next phase of the project. For real samples with unknown DNA concentration, we will first reduce the risk of DNA loss by improving the passivation process and then assess the minimal required quantity of carrier DNA that will not interfere with any concentrations of DNA samples.

Lab on a Chip Accepted Manuscript

In conclusion, for the first time, ultrafast rtPCR can be performed in less than 7 minutes while conserving the amplification efficiency, sensitivity and large-volume of conventional commercial rtPCR systems, thus opening the way to the development of user-friendly POC molecular analyses carried out directly by practitioners.

**Acknowledgments**

This work was supported by the ANR-DGA, BPI France and European Commission through respectively funding ASTRID n°ANR-11-ASTR-0019-01, AIMA Laboratoire n°A1402022 Q and FP7-PEOPLE-2013-ITN – Marie-Curie Action: LAPASO grant agreement n°607350. The authors thank Alice Pinheiro and François Radvanyi (Institut Curie) for their collaborations, technical advices and support; Yohan Farouz, Diana Molino, Jacques Fattacioli (École Normale Supérieure de Paris) for the fruitful discussions and advices; Guilhem Larigauderie and the DGA, CBRN Defense for providing biological samples and reagents; Damien Baigl and the technical department of the École Normale Supérieure de Paris for technical support and help; Sage Morghan for the English proofreading of the manuscript.

Lab on a Chip Accepted Manuscript

**Legends to figures**

**Figure 1:** rtPCR microfluidic chip and experimental set-up: (a) Schematic cross-section of the device, (b) Top view photograph of microfluidic chip with the microfluidic thermalization chamber filled with dyed water, (c) Photograph of the microfluidic chip and the heat exchangers during temperature characterization with an infra-red thermometer, (d) Diagram of the experimental set-up for ultrafast rtPCR, (e) Photograph of the microfluidic chip placed above the fluorescence measuring system.

**Figure 2:** Performances of microfluidic thermalization. (a) Temperature during thermocycling for ultrafast rtPCR (30 cycles in 2 min). (b) Temperature homogeneity of microfluidic thermalization during the heating phase.

**Figure 3:** rtPCR and RT-rtPCR time optimization. (a) Influence of annealing-elongation time on Ct values of rtPCR done with SYBR Green and probe fluorescent reporters. (b) Comparison of amplification curves for short or long rtPCR times with SYBR Green or probes reporters (anthrax simulating agent detection). (c) Influence of reverse transcription time on RT-rtPCR Ct.

**Figure 4:** Comparison of amplification curves made with microfluidic thermalization and commercial system (40 cycles). R.F.U. stands for Relative Fluorescence Units $= \frac{(x(t)-x(0))}{(x(final)-x(0))} \times 100$. (a) Detection of anthrax simulating agent by rtPCR and (b) Detection of Ebola simulating agent by RT-rtPCR, (c) Dependence of Ct on dilution factor assessing rtPCR efficiency and sensitivity.

**Figure 5:** Ultrafast rtPCR melting curve analysis. (a) Fluorescence evolution in function of temperature. (b) Derivative of fluorescence in function of temperature.

Lab on a Chip Accepted Manuscript

**Figure 6:** Comparison of rtPCR amplification curves made with different amplicon sizes and rtPCR durations showing amplicon size distinction by ultrafast rtPCR.

Lab on a Chip Accepted Manuscript

## References


1 D. Butler, *Nature*, 2014, 516, 154–155.

2 Nature News, *Nature*, 2015, 518, 460–461.

3 W. Chen, B. He, C. Li, X. Zhang, W. Wu, X. Yin, B. Fan, X. Fan and J. Wang, *J. Med. Microbiol.*, 2007, 56, 603–607.

4 K. V. Mohan, K. G. Murugavel, Rajanikanth, S. Mathews, K. Raghuram, P. Rajasambandam, A. Murali, U. Srinivas, Mathiazhagan, K. R. Palaniswamy, S. K. Panda and S. P. Thyagarajan, *Indian J. Gastroenterol.*, 1999, 18, 73–75.

5 L. Durnez, W. Van Bortel, L. Denis, P. Roelants, A. Veracx, H. D. Trung, T. Sochantha and M. Coosemans, *Malaria J.*, 2011, 10, 195.

6 I. M. Mackay, K. E. Arden and A. Nitsche, *Nucleic Acids Res.*, 2002, 30, 1292–1305.

7 M. J. Espy, J. R. Uhl, L. M. Sloan, S. P. Buckwalter, M. F. Jones, E. A. Vetter, J. D. C. Yao, N. L. Wengenack, J. E. Rosenblatt, F. R. Cockerill and T. F. Smith, *Clin. Microbiol. Rev.*, 2006, 19, 165–256.

8 D. Fraga, T. Meulia and S. Fenster, in *Current Protocols Essential Laboratory Techniques*, John Wiley & Sons, Inc., 2008.

9 G. Wong, I. Wong, K. Chan, Y. Hsieh and S. Wong, *PLoS ONE*, 2015, 10(7): e0131701.

10 World Health Organization, Urgently needed: rapid, sensitive, safe & simple diagnostic tests, http://www.who.int/medicines/ebola-treatment/2014-1107_Call_for_Diagnostics.pdf?ua=1 and http://www.who.int/mediacentre/news/ebola/18-november-2014-diagnostics/en/ (accessed February 2016).

11 D. S. Chertow, C. Kleine, J. K. Edwards, R. Scaini, R. Giuliani and A. Sprecher, *N. Engl. J. Med.*, 2014, 371, 2054–2057.

12 C.-M. Chang, W.-H. Chang, C.-H. Wang, J.-H. Wang, J. D. Mai and G.-B. Lee, *Lab Chip*, 2013, 13, 1225–1242.

13 Y. Sun, T. L. Quyen, T. Q. Hung, W. H. Chin, A. Wolff and D. D. Bang, *Lab Chip*, 2015, 15, 1898–1904.

14 Z. Ma, R. W. Lee, B. Li, P. Kenney, Y. Wang, J. Erikson, S. Goyal and K. Lao, *Proc. Natl. Acad. Sci.*, 2013, 110, 14320–14323.

15 D. Moschou, N. Vourdas, G. Kokkoris, G. Papadakis, J. Parthenios, S. Chatzandroulis and A. Tserepi, *Sens. Actuators B Chem.*, 2014, 199, 470–478.

16 Y. Fuchiwaki, H. Nagai, M. Saito and E. Tamiya, *Biosens. Bioelectron.*, 2011, 27, 88–94.


Lab on a Chip Accepted Manuscript

17 S. Brunklaus, T. E. Hansen-Hagge, J. Erwes, J. Höth, M. Jung, D. Latta, X. Strobach, C. Winkler, M. Ritzi-Lehnert and K. S. Drese, *Electrophoresis*, 2012, 33, 3222–3228.

18 P. Neuzil, C. Zhang, J. Pipper, S. Oh and L. Zhuo, *Nucleic Acids Res.*, 2006, 34, e77–e77.

19 H. Kim, S. Dixit, C. J. Green and G. W. Faris, *Opt. Express*, 2009, 17, 218–227.

20 E. K. Wheeler, C. A. Hara, J. Frank, J. Deotte, S. B. Hall, W. Benett, C. Spadaccini and N. R. Beer, *Analyst*, 2011, 136, 3707–3712.

21 H. Terazono, H. Takei, A. Hattori and K. Yasuda, *Jpn. J. Appl. Phys.*, 2010, 49, 06GM05.

22 BJS Technologies, XXpress, http://www.xxpresspcr.com/ (accessed February 2016).

23 Y.-K. Cho, J. Kim, Y. Lee, Y.-A. Kim, K. Namkoong, H. Lim, K. W. Oh, S. Kim, J. Han, C. Park, Y. E. Pak, C.-S. Ki, J. R. Choi, H.-K. Myeong and C. Ko, *Biosens. Bioelectron.*, 2006, 21, 2161–2169.

24 M.-S. Yoo, K. C. N. Thi, P. Van Nguyen, S.-H. Han, S.-H. Kwon and B.-S. Yoon, *J. Virol. Methods*, 2012, 179, 195–200.

25 Analytik Jena, qTower, http://www.analytik-jena.de/fr/life-science/products/products-dynamic/cat/real-time-rapidpcr/prod/qtower.html (accessed February 2016).

26 H.-O. Song, J.-H. Kim, H.-S. Ryu, D.-H. Lee, S.-J. Kim, D.-J. Kim, I. B. Suh, D. Y. Choi, K.-H. In, S.-W. Kim and H. Park, *PLoS One*, 2012, 7, e53325.

27 Cepheid, GeneXpert system, http://www.cepheid.com/us/cepheid-solutions/systems/genexpert-systems/genexpert-i (accessed February 2016).

28 R. Abdul Khaliq, R. Kafafy, H. M. Salleh and W. F. Faris, *Nanotechnology*, 2012, 23, 455106.

29 I. Erill, S. Campoy, J. Rus, L. Fonseca, A. Ivorra, Z. Navarro, J. A. Plaza, J. Aguiló and J. Barbé, *J. Micromechanics Microengineering*, 2004, 14, 1558.

30 J. Noh, S. W. Sung, M. K. Jeon, S. H. Kim, L. P. Lee and S. I. Woo, *Sens. Actuators Phys.*, 2005, 122, 196–202.

31 R. P. Oda, M. A. Strausbauch, A. F. R. Huhmer, N. Borson, S. R. Jurrens, J. Craighead, P. J. Wettstein, B. Eckloff, B. Kline and J. P. Landers, *Anal. Chem.*, 1998, 70, 4361–4368.

32 J. R. Peham, L.-M. Recnik, W. Grienauer, M. J. Vellekoop, C. Nöhammer and H. Wiesinger-Mayr, *Microsyst. Technol.*, 2011, 18, 311–318.

33 A. J. De Mello, *Lab Chip*, 2001, 1, 24N–29N.

34 X. Qiu, M. G. Mauk, D. Chen, C. Liu and H. H. Bau, *Lab Chip*, 2010, 10, 3170–3177.

Lab on a Chip Accepted Manuscript

35 D. Rawer, A. Borkhardt, M. Wilda, S. Kropf and J. Kreuder, *Leukemia,* 2003, 17, 2527–2528.

36 P. Rossmanith and M. Wagner, *J. Food Prot.*, 2011, 74, 1404–1412.

37 J. Kim, M. Mauk, D. Chen, X. Qiu, J. Kim, B. Gale and H. H. Bau, *Analyst*, 2010, 135, 2408–2414.

38 D. Chen, M. Mauk, X. Qiu, C. Liu, J. Kim, S. Ramprasad, S. Ongagna, W. R. Abrams, D. Malamud, P. L. A. M. Corstjens and H. H. Bau, *Biomed. Microdevices*, 2010, 12, 705–719.

39 J. Kim, D. Byun, M. G. Mauk and H. H. Bau, *Lab Chip*, 2009, 9, 606–612.

40 N. Crews, C. Wittwer, R. Palais and B. Gale, *Lab Chip*, 2008, 8, 919–924.

41 C. J. Easley, J. A. C. Humphrey and J. P. Landers, *J. Micromechanics Microengineering*, 2007, 17, 1758.

42 G. Maltezos, M. Johnston, K. Taganov, C. Srichantaratsamee, J. Gorman, D. Baltimore, W. Chantratita and A. Scherer, *Appl. Phys. Lett.*, 2010, 97, 264101.

43 Y. Xia and G. M. Whitesides, *Angew. Chem. Int. Ed.*, 1998, 37, 550–575.

44 A.-N. Spiess, C. Feig and C. Ritz, *BMC Bioinformatics*, 2008, 9, 221.

45 R. Rasmussen, in *Rapid Cycle Real-Time PCR*, eds. P. D. med S. Meuer, P. D. C. Wittwer and D. K.-I. Nakagawara, Springer Berlin Heidelberg, 2001, pp. 21–34.

46 C. T. Wittwer and D. J. Garling, *BioTechniques*, 1991, 10, 76–83.

47 J. L. Montgomery and C. T. Wittwer, *Clin. Chem.*, 2014, 60, 334–340.

48 I. V. Kutyavin, *Nucleic Acids Res.*, 2010, 38, e29–e29.

49 US Pat., 20040053254 A1, 2004.

50 H. Zipper, H. Brunner, J. Bernhagen and F. Vitzthum, *Nucleic Acids Res.*, 2004, 32, e103.

51 D. Lee, P.-J. Chen and G.-B. Lee, *Biosens. Bioelectron.*, 2010, 25, 1820–1824.

52 S. Kirchner, K. M. Krämer, M. Schulze, D. Pauly, D. Jacob, F. Gessler, A. Nitsche, B. G. Dorner and M. B. Dorner, *Appl. Environ. Microbiol.*, 2010, 76, 4387–4395.

53 M. Liew, R. Pryor, R. Palais, C. Meadows, M. Erali, E. Lyon and C. Wittwer, *Clin. Chem.*, 2004, 50, 1156–1164.

54 uMELT, https://www.dna.utah.edu/umelt/umelt.html (accessed February 2016).

55 Oligonucleotide Properties Calculator, http://www.basic.northwestern.edu/biotools/oligocalc.html (accessed February 2016).


Lab on a Chip Accepted Manuscript

56 T. A. Taton, C. A. Mirkin and R. L. Letsinger, *Science*, 2000, 289, 1757–1760.

57 M. C. Edwards and R. A. Gibbs, *Genome Res.*, 1994, 3, S65–S75.

Lab on a Chip Accepted Manuscript

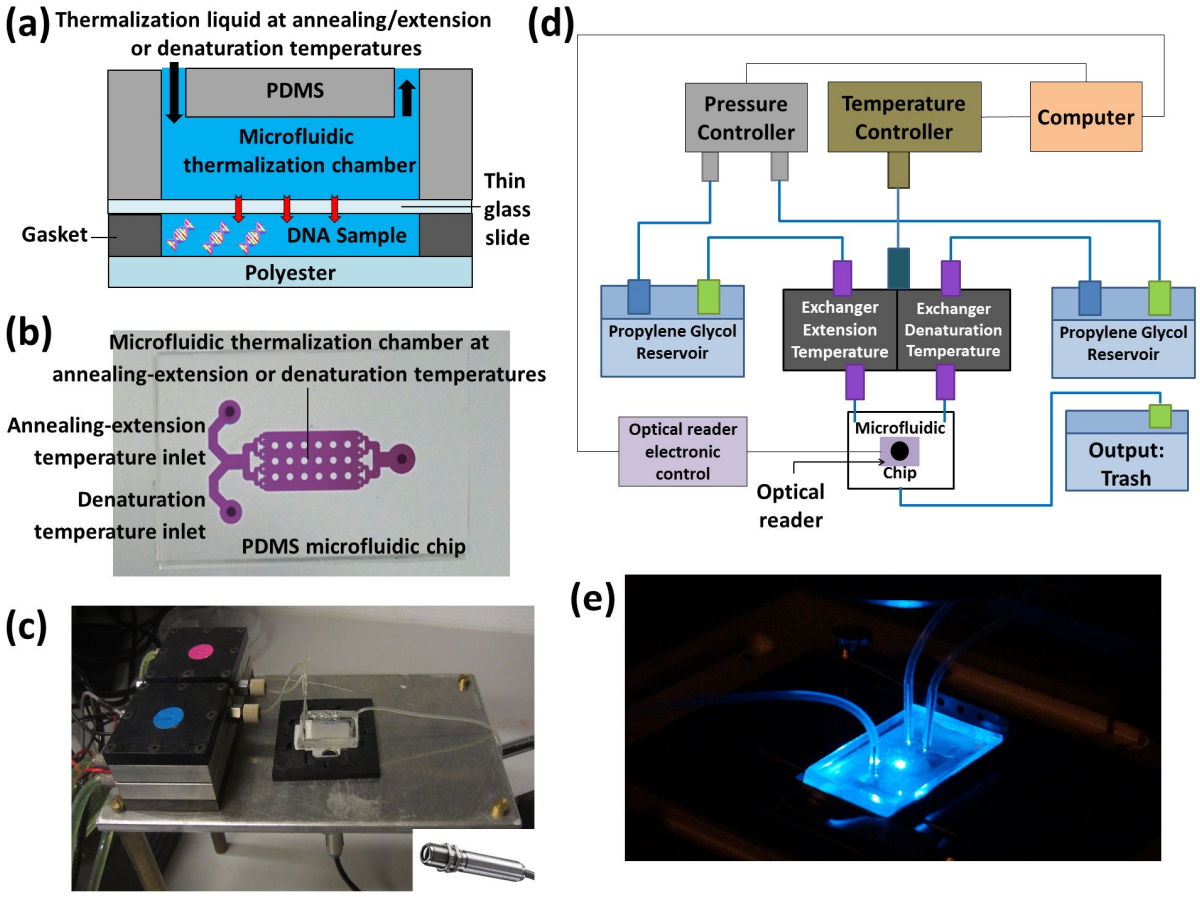


Figure 1

Lab on a Chip Accepted Manuscript

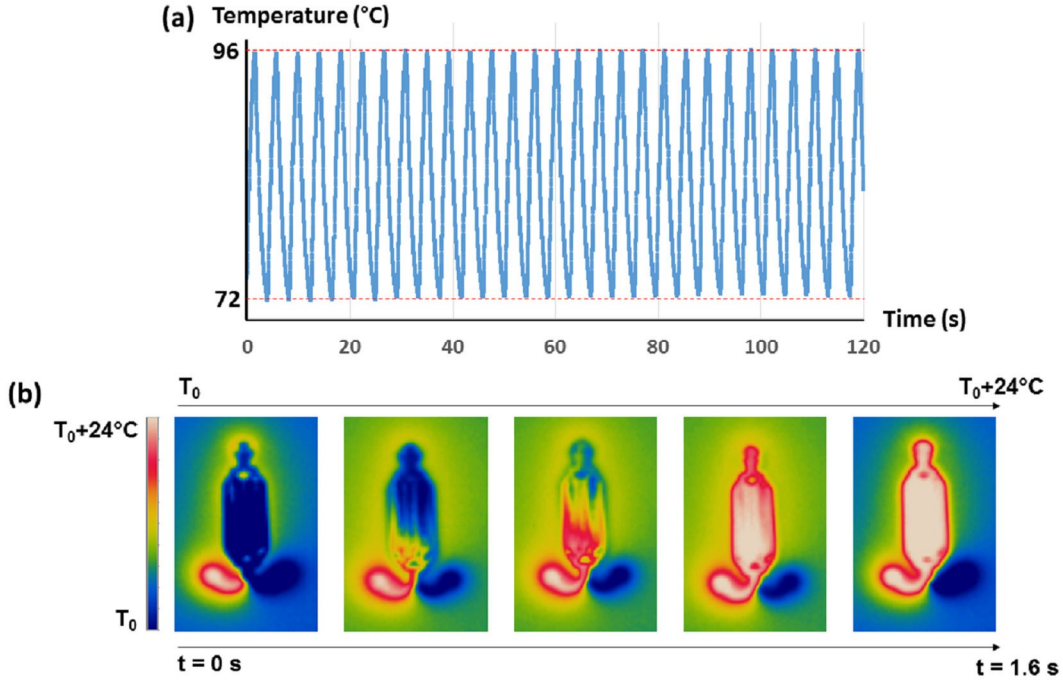


Figure 2

Lab on a Chip Accepted Manuscript

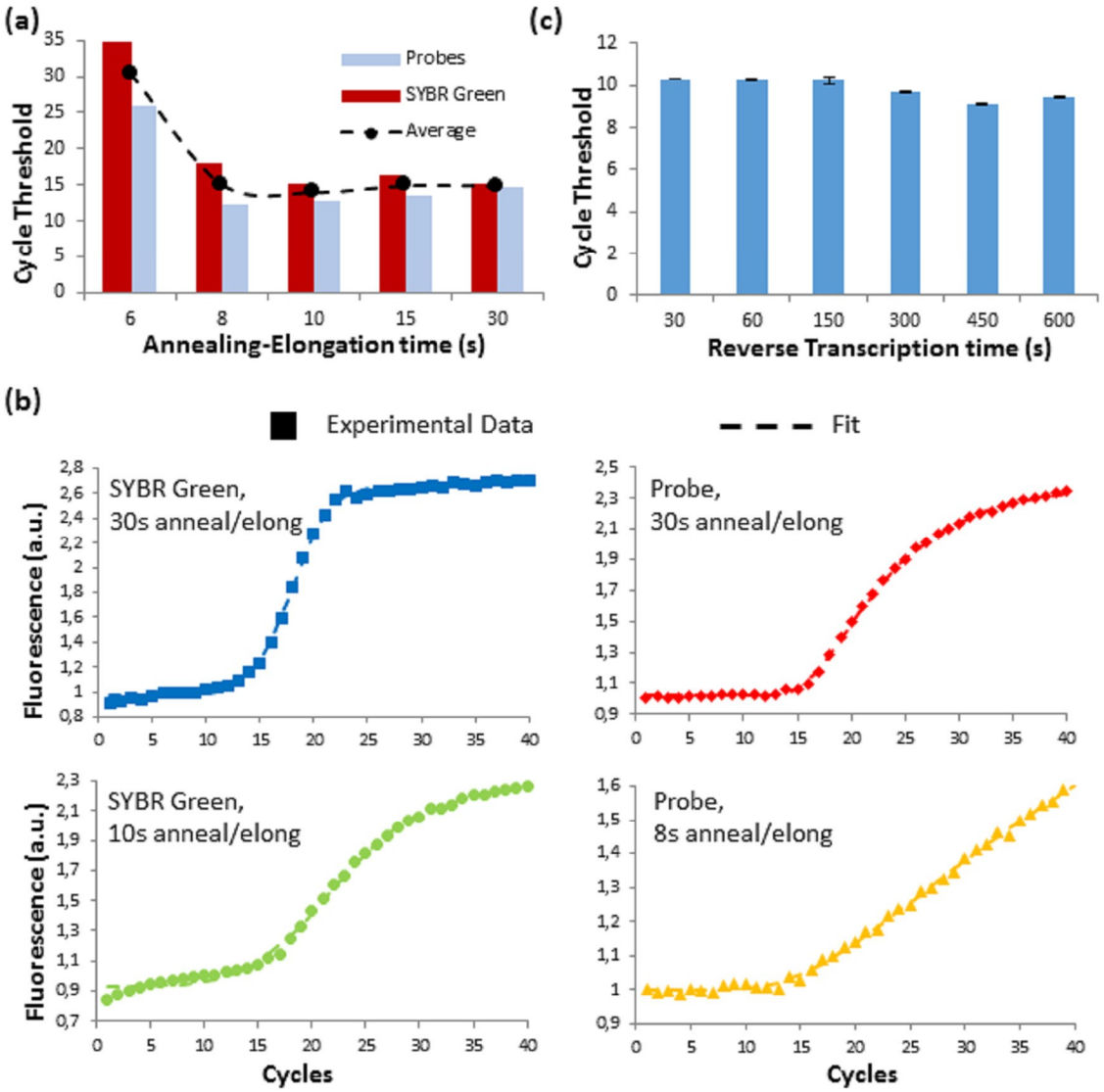


Figure 3

Lab on a Chip Accepted Manuscript

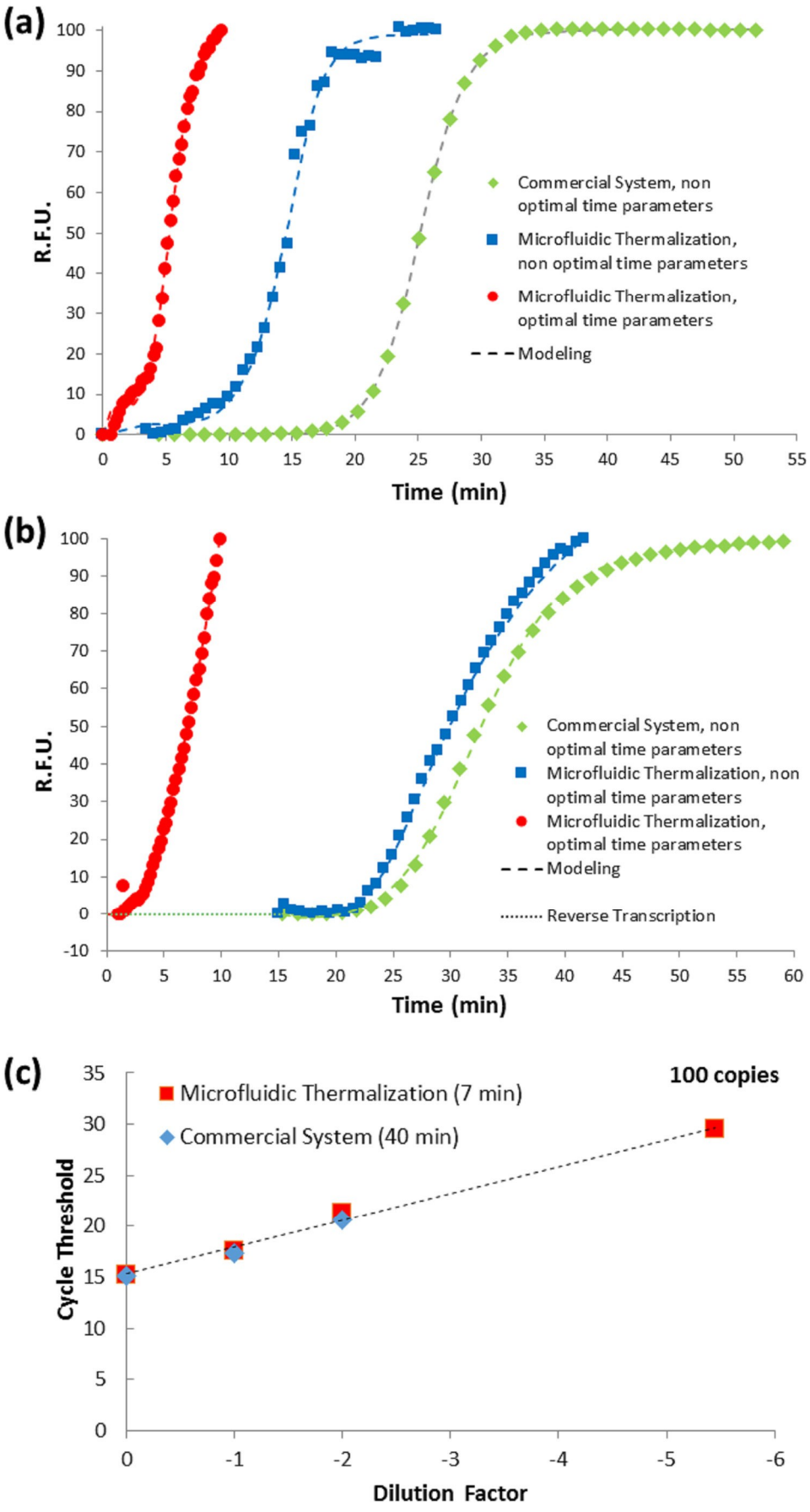


Figure 4

Lab on a Chip Accepted Manuscript

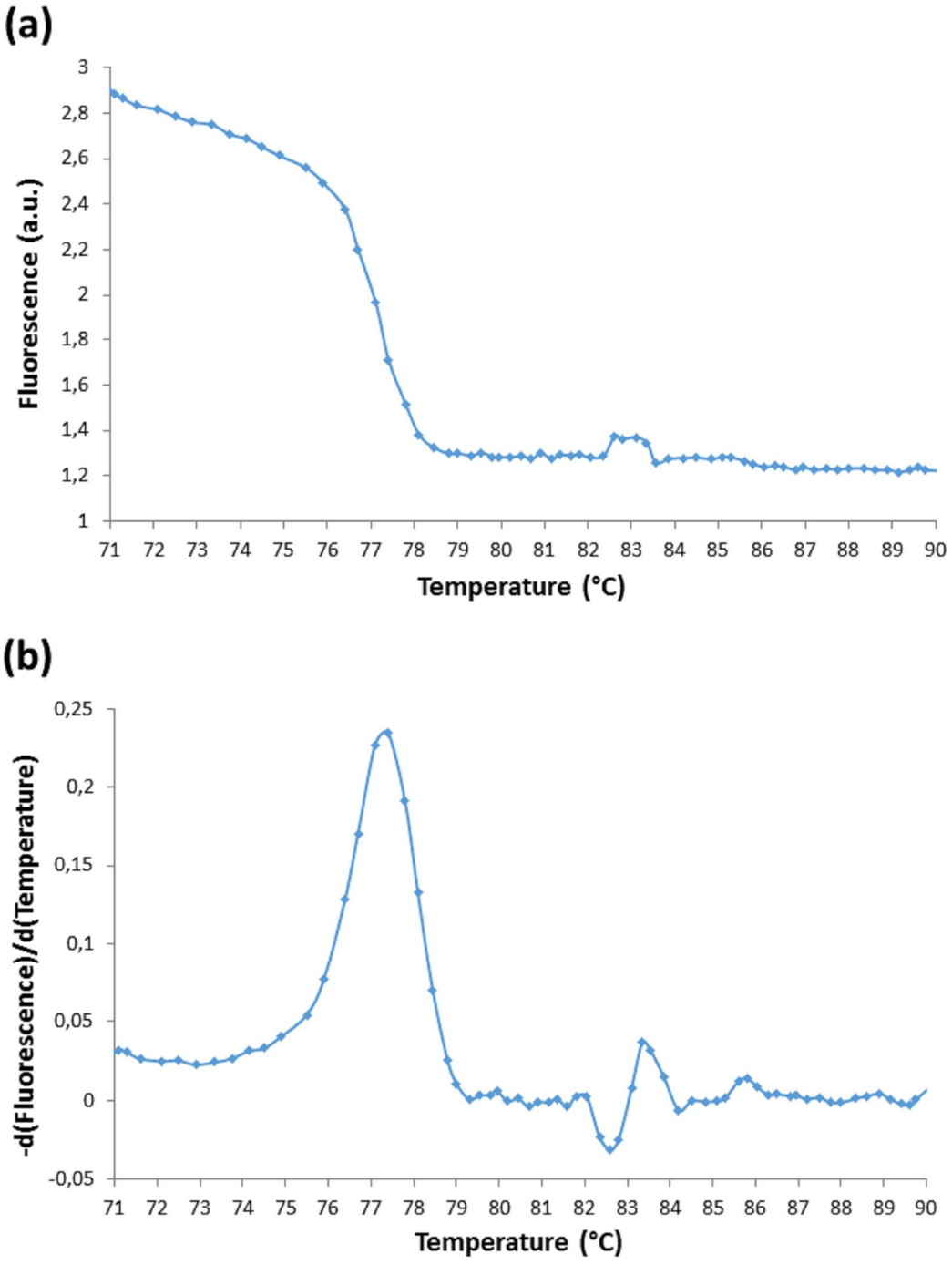


Figure 5

Lab on a Chip Accepted Manuscript

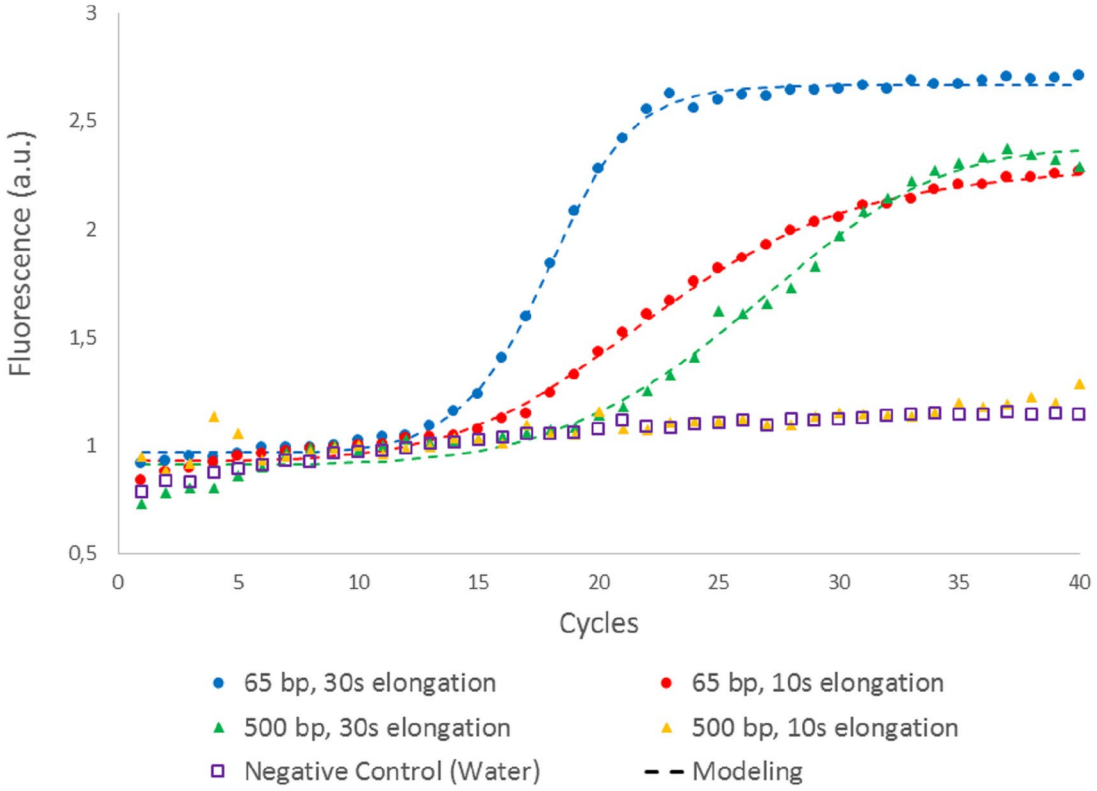


Figure 6

Lab on a Chip Accepted Manuscript